

Article

# Novel Characterization Techniques for Additive Manufacturing Powder Feedstock

Benjamin Young <sup>1</sup>, Joseph Heelan <sup>1</sup>, Sean Langan <sup>1</sup>, Matthew Siopis <sup>2</sup>, Caitlin Walde <sup>1,\*</sup>  and Aaron Birt <sup>1</sup>

<sup>1</sup> Solvus Global, Worcester, MA 01605, USA; Benjamin.young@solvusglobal.com (B.Y.); joseph.heelan@solvusglobal.com (J.H.); sean.langan@solvusglobal.com (S.L.); aaron.birt@solvusglobal.com (A.B.)

<sup>2</sup> US Army Research Laboratory, Aberdeen Proving Ground, Aberdeen, MD 21005, USA; matthew.j.siopis.civ@mail.mil

\* Correspondence: Caitlin.walde@solvusglobal.com; Tel.: +1-508-373-2750

**Abstract:** Additive manufacturing is a rapidly expanding field, encompassing many methods to manufacture parts and coatings with a wide variety of feedstock. Metal powders are one such feedstock, with a range of compositions and morphologies. Understanding subtle changes in the feedstock is critical to ensure successful consolidation and quality control of both the feedstock and manufactured part. Current standards lack the ability to finely distinguish almost acceptable powders from barely acceptable ones. Here, novel means of powder feedstock characterization for quality control are demonstrated for the solid-state AM process of cold spray, though similar methods may be extrapolated to other additive methods as well. These characterization methods aim to capture the physics of the process, which in cold spray consists of high strain rate deformation of solid-state feedstock. To capture this, in this effort powder compaction was evaluated via rapidly applied loads, flowability of otherwise non-flowable powders was evaluated with the addition of vibration, and powder electrical resistivity was evaluated through compaction between two electrodes. Several powders, including aluminum alloys, chromium, and cermet composites, were evaluated in this effort, with each case study demonstrating the need for non-traditional characterization metrics as a means of quality control and classification of these materials.

**Keywords:** additive manufacturing; metal powders; cermet powders; characterization; cold spray



**Citation:** Young, B.; Heelan, J.; Langan, S.; Siopis, M.; Walde, C.; Birt, A. Novel Characterization Techniques for Additive Manufacturing Powder Feedstock. *Metals* **2021**, *11*, 720. <https://doi.org/10.3390/met11050720>

Academic Editor: Francisco Paula Gómez Cuevas

Received: 31 March 2021  
Accepted: 23 April 2021  
Published: 27 April 2021

**Publisher's Note:** MDPI stays neutral with regard to jurisdictional claims in published maps and institutional affiliations.



**Copyright:** © 2021 by the authors. Licensee MDPI, Basel, Switzerland. This article is an open access article distributed under the terms and conditions of the Creative Commons Attribution (CC BY) license (<https://creativecommons.org/licenses/by/4.0/>).

## 1. Introduction

Additive manufacturing has made significant advancements in recent years and has taken center stage in the manufacturing world. With the ability to manufacture net shape components and touting strong cost savings for R&D and low production batches, it has proven its usefulness over the challenges of traditional manufacturing. However, additive manufacturing is not without its own set of challenges. Part anisotropy and dependence on build orientation require additional research and development to evaluate and optimize and need to be considered for quality control [1]. Additionally, build rates can be slow and build envelopes small, especially when compared to full-scale production of large parts, potentially limiting applications [2]. Finally, while AM processes generally produce less waste than traditional subtractive manufacturing, feedstock can be very expensive and there is still a portion of feedstock wasted. As the effects of process parameters on reclaimed feedstock are still relatively unknown, much work remains to effectively reclaim and potentially reuse this feedstock [3–7]. Recognizing these challenges, organizations such as the US Department of Defense (DoD), US Department of Energy (DoE), US National Air and Space Administration (NASA), US Food and Drug Administration (USFDA), and the National Institute of Standards and Technology (NIST) have all recognized that part qualification and certification will be the underlying challenge and must be addressed moving forward if additive manufacturing is to be widely implemented [8–11].

Post-process inspection and in-process monitoring have been a major focus for development in recent years. This work discusses quality control of a less explored but equally important process component: the feedstock. The effect of variable feedstock on consolidated parts has been evaluated for a wide variety of materials on many additive manufacturing platforms [12]. This boils down to the need for quality control and the need to quantify acceptable bounds for manufacturing parameters. Currently, evaluating feedstock performance in an AM process is performed through an Edisonian trial-and-error approach. This approach is time consuming and does not lend itself well to the identification of key feedstock features or to the development of standards around those key features.

This work demonstrates the utility of three novel powder feedstock characterization methods to more accurately predict feedstock behavior in the additive manufacturing process of cold spray. These methods can help establish meaningful standards for individual material-application combinations, can be used to develop quality control metrics, and can be used as a pre-screening tool for novel materials for an application.

Cold spray specifically is a solid-state additive manufacturing process whereby powder feedstock is accelerated by a carrier gas through a converging diverging nozzle to supersonic velocities towards a substrate, where the particles deform, adhere, and build up layers [13]. It is capable of depositing a variety of materials, including aluminum and aluminum alloys, steels, refractory metals, cermets, and polymers. As cold spray is a solid-state process, any microstructural features or defects present in the feedstock are retained in the consolidated part as well. This can be advantageous when designing feedstock, but can also be difficult for quality control, as it requires tight tolerances.

Current means to control quality in feedstock for additive manufacturing center around flowability and sizing [14–17]. While flowability is an important metric in cold spray as powders must be able to flow in the powder feeder and through the system, current standards fail to capture the nuances of the cold spray system. If all other factors are equal, a more flowable powder will be more easily cold sprayed than a non-flowing powder. Two of the most popular methods for measuring flowability are Hall Flow and Carney flow [14,15]. Both involve measuring the amount of time it takes for a set amount of powder to flow through a funnel. What is lacking with these methods, however, is that it is possible to cold spray powders of low flowability, that might not flow through either the Hall or the Carney funnel. In cold spray, this can be accomplished through the use of mechanical vibration with feeding [18–20].

Alternative means to evaluate powder materials have been used in the literature but have not been incorporated to standards. Powder compressibility is one such method. In this, powder is placed between two electrodes, pressure is applied, and the resistivity of the powder is measured. Historically this has been used to examine metallic powders with oxide coatings [21], the effect of porosity on the resistivity of titanium powders [22], and the resistivity of metal oxide-activated carbon nanocomposites [23]. Multiple pressures can be used, and curves for resistivity as a function of pressure can be generated. In the AM space, surface oxides and powder porosity can greatly affect the quality of the manufactured part. In cold spray specifically, surface oxides can affect particle deposition and bonding and reduce the overall strength of the deposited material, and are not easily detected via size or flowability [24,25].

While control over feedstock is important in all AM processes, it is especially so for a solid state process such as cold spray. Recently, there has been considerable interest in enhancing the ability to characterize this feedstock. Recently, machine learning and computer vision were applied to powder for AM, and achieved more than 95% accuracy at segregating commercial powders into their correct material systems [26]. Furthermore, nanoindentation was successfully used to characterize cold spray feedstock [27]. Cano et al. recently used powder properties as part of a comprehensive study on cold spray with optimization software [28]. Cote et al. recently performed extensive characterization of gas-atomized Al 5056 powders, showing that the powder had been experiencing aging

effects [29]. The same group also examined using machine learning to examine powder flowability, and found an accuracy of 98.04% [30]. This is an area that will continue to grow as it has such a large effect on the final AM product, and there are still large advances to be made.

Feedstock evaluation techniques that can indicate potential differences in powders similar in size and flowability prior to use in AM processes can save time and development costs. In this work, a series of case studies of various powders for cold spray applications are used to demonstrate the need for novel characterization techniques. These case studies include (1) the ability to detect small compositional differences in CrC wear powders for quality control; (2) the ability to detect the effect of processing on a low-flowability Cr powder; and (3) the ability to differentiate between pre-processing conditions of aluminum powder. Together, they can be used to better understand feedstock powders and work to predict AM performance.

Finally, not all AM processes are the same, and differences in process drive different performance metrics that should be measured of the feedstock. For example, in cold spray the primary physical phenomenon is high strain rate deformation whereas in laser powder beds the primary phenomenon is the consumption of powder by a melt pool. Monitoring the physics of feedstock powder before its use in the manufacturing process gives greater quality control than simply measuring default characteristics. The extra techniques utilized here aim to measure and evaluate the physics of the process to ensure that similar phenomena are captured.

## 2. Materials and Methods

### 2.1. Materials

A variety of commercially available powders were evaluated as part of this study as a means to demonstrate the utility of the novel characterization methods relevant to cold spray. Each powder is discussed in the following sections relevant to each case study. To maintain impartiality, powders are identified by their composition, size, and morphology, rather than by vendor. Powders were broadly characterized for their size, morphology, and density. The particle size distribution was determined via a static image analysis method compliant with ISO 13322-1, densities (apparent, tapped, and Hausner ratio) were evaluated via ASTM B527-20, and morphology was determined via scanning electron microscopy (SEM) analysis of loose powder using a tungsten-source SEM (FEI Quanta 600) [31,32].

#### 2.1.1. Quality Control of Cermet Powder Blends

For this case study, commercially available WIP-C1 and WIP-C2 chrome carbide-based powders were evaluated. WIP-C1 is chrome carbide nickel of the composition Cr-31Ni-3C, and WIP-C2 is chrome carbide nickel chrome of the composition Cr-26Ni-3C. As both are agglomerated chromium-carbide nickel powders, these powders have proven to be difficult to distinguish via traditional methods, and hence their evaluation via the novel methods discussed here. Powders were broadly characterized for their size, morphology, and density; these values are reported in Table 1. Example SEM micrographs for each powder can be seen in Figures 1 and 2; full composition can be seen in Table 2.

**Table 1.** General characterization metrics for the WIP powders considered in this study.

Powder	Morphology	D <sub>10</sub> ( $\mu\text{m}$ )	D <sub>50</sub> ( $\mu\text{m}$ )	D <sub>90</sub> ( $\mu\text{m}$ )	Apparent Density (g/mL)	Tapped Density (g/mL)	Hausner Ratio
WIP-C1	Agglomerate	18.0	28.0	41.2	3.9	4.4	1.1
WIP-C2	Agglomerate	19.1	30.7	45.7	4.0	4.5	1.1

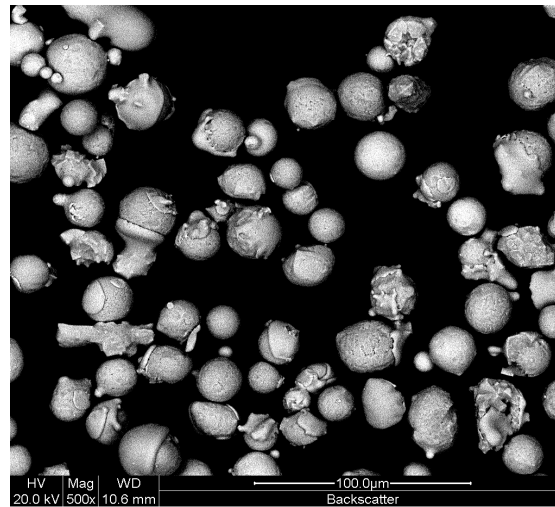


Figure 1. BSE image of WIP-C1 powder.

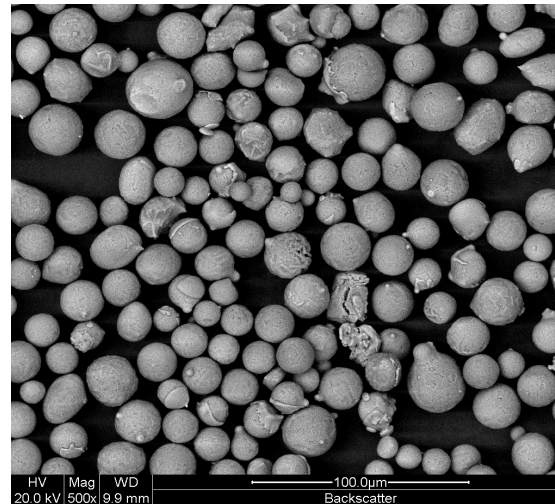


Figure 2. BSE image of WIP-C2 powder.

Table 2. Composition of WIP powders.

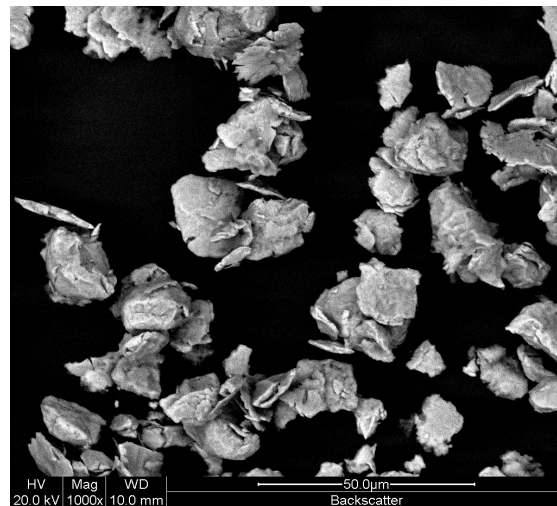
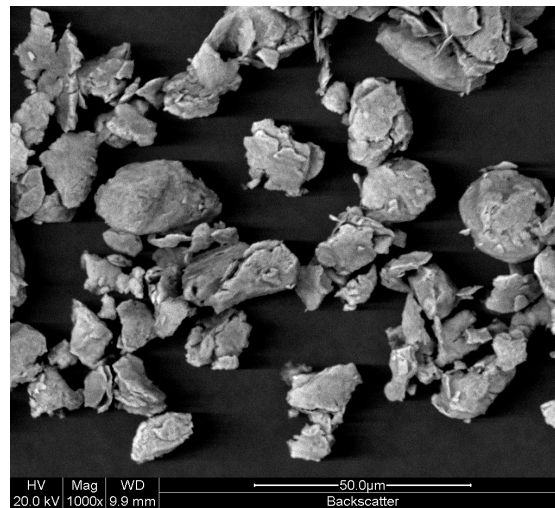
Element Concentration (wt%)	Co	Cr	Fe	Ni	W	Al	B	Mo	Si	V	C
WIP-C1	0.02	68.45	0.08	27.84	0.01	0.06	0.04	0.01	0.43	0.01	3.00
WIP-C2	0.01	72.01	0.08	24.35	0.01	0.07	0.04	0.01	0.39	0.01	2.94

### 2.1.2. Pre-Processing of Chromium Powder

For this case study, commercially available chromium powder was evaluated in the un-processed and dried conditions. Size, morphology, and density values are reported in Table 3. The dried chromium was dried at 60 °C for 24 h. Example SEM micrographs for each powder can be seen in Figures 3 and 4, and composition of the Cr powders can be seen in Table 4.

**Table 3.** General characterization metrics for the Cr powders considered in this study.

Powder	Morphology	D <sub>10</sub> ( $\mu\text{m}$ )	D <sub>50</sub> ( $\mu\text{m}$ )	D <sub>90</sub> ( $\mu\text{m}$ )	Apparent Density (g/mL)	Tapped Density (g/mL)	Hausner Ratio
Un-processed Chromium	Irregular	9.8	16.9	24.0	2.2	3.2	1.5
Dried Chromium	Irregular	9.6	16.3	23.4	2.5	3.4	1.3

**Figure 3.** BSE image of unprocessed Cr powder.**Figure 4.** BSE image of dried Cr powder.**Table 4.** Composition of Cr powder.

Element	Cr	O	N	Si	C	Ni	Other
Concentration (ppm)	Bal	1900	310	180	62	19	<2115

### 2.1.3. Pre-Processing of Aluminum 6061

For this case study, commercially available gas atomized aluminum 6061 powder was evaluated at three different oxygen content levels; these were high, medium, and low as shown in Figure 5. Oxygen content was determined by inert gas fusion using ASTM E1019-18. In additive manufacturing, powder pre-processing can include heat treatments

or drying techniques that will change oxygen content but have little effect on other powder attributes. This case study serves to evaluate the sensitivity of 6061 powder to specific processing conditions and the ability of the novel characterization metrics to detect that sensitivity. Particle size, morphology, and density for each condition are reported in Table 5. Example SEM micrographs for each powder can be seen in Figure 6, Figure 7, and Figure 8; composition for the 6061 powder is shown in Table 6 and oxygen content specifically is shown in Figure 5.

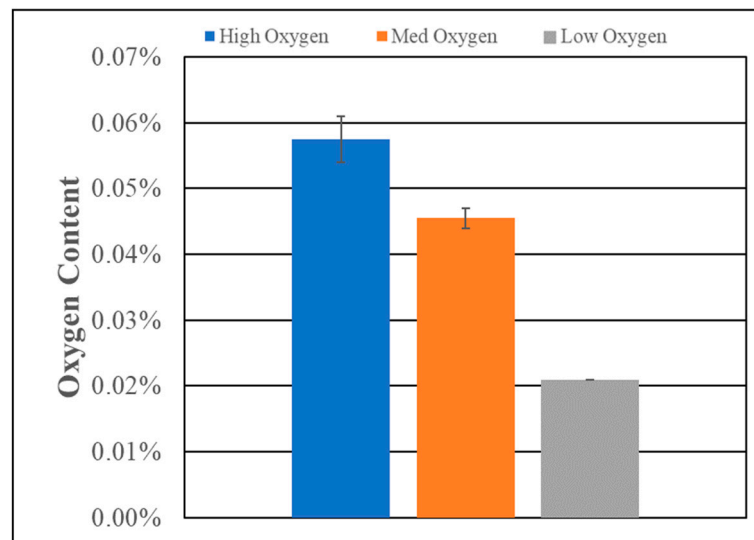


Figure 5. Oxygen content of evaluated aluminum powders.

Table 5. General characterization metrics for the aluminum powders considered in this study.

Powder	Morphology	D <sub>10</sub> (μm)	D <sub>50</sub> (μm)	D <sub>90</sub> (μm)	Apparent Density (g/mL)	Tapped Density (g/mL)	Hausner Ratio
High O 6061	Spherical	23.0	34.6	53.8	1.3	1.6	1.2
Med O 6061	Spherical	23.0	34.3	54.2	1.3	1.6	1.2
Low O 6061	Spherical	22.8	33.9	55.5	1.3	1.6	1.2

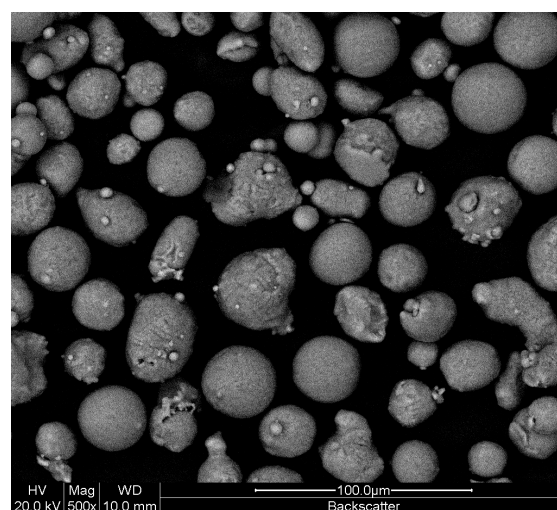


Figure 6. BSE image of high oxygen Al powder.

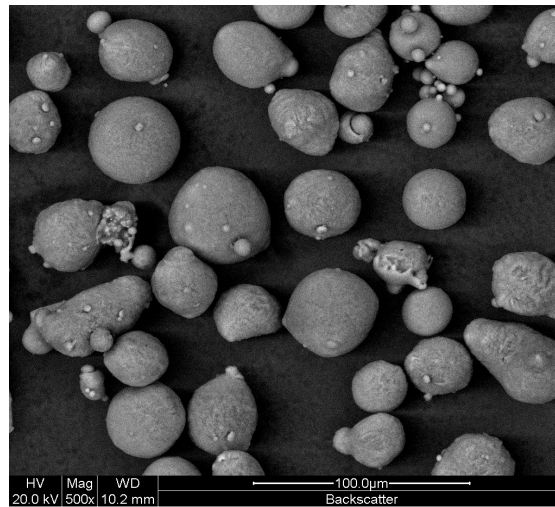


Figure 7. BSE image of med oxygen Al powder.

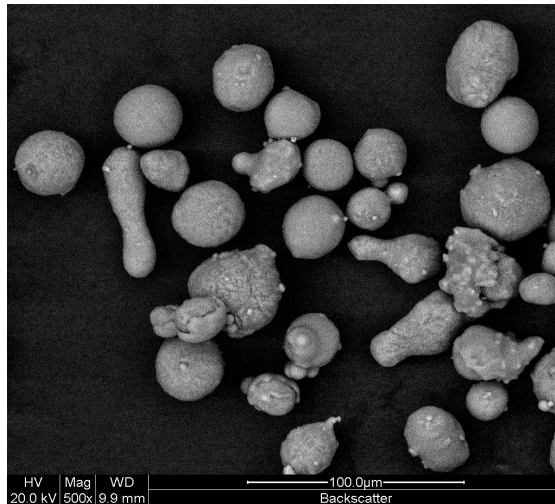


Figure 8. BSE image of low oxygen Al powder.

Table 6. Composition of Al powder.

Element	Cr	Cu	Fe	Mg	Mn	Si	Ti	Zn	Other	Al
Concentration (wt%)	0.11	0.28	0.11	0.98	0.0043	0.61	0.01	0.014	<0.20	Bal

## 2.2. Characterization

### 2.2.1. Flowability

Flowability of the powders considered in this work was evaluated via Carney flow and Hall flow, as well as a modified, vibrated Hall flow [14,15]. In the latter method, a commercially available vibrator motor (DC 6V, 6800RPM, 31 mm by 24 mm diameter, Xingdong Environmental Ventilation Engineering, Dongguan, China) was attached to the Hall funnel via a clamp ring as shown in Figure 9. Powder was loaded into the funnel with the orifice closed, and the vibration was initiated when the orifice was opened. Flow rate was recorded as a function of time and time to empty funnel was calculated and compared to the standard Hall and Carney flow metrics. Tests were completed six times per sample.

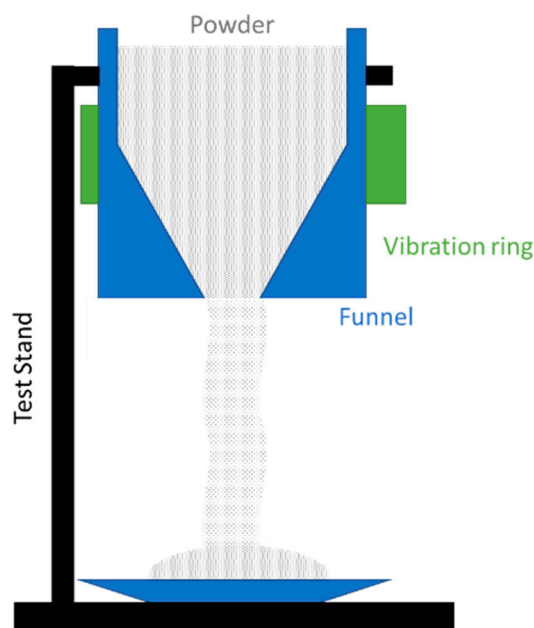


Figure 9. Schematic showing cross section of vibrational flowability test.

Analysis was performed at a single vibration level, and additional work could be done to evaluate the effect of varying vibration parameters on the flowability of the powder. The effort here aimed to show the utility of including such a test when evaluating low flowability powders for use in the cold spray process and additional work will be performed to evaluate the relationship between powder attributes such as size, varied vibrational conditions, and the resultant flow properties.

The level of accuracy for this proposed method is dependent upon the resolution of the timer and the scale; as the input mass does not change over time during testing, the accuracy with the equipment used here is expected to be  $\pm 0.095$  s.

### 2.2.2. Compressibility

Figure 10 shows a schematic of a cross section of the apparatus used to evaluate powder compressibility. A total of 1.8 mL (tapped) of powder was loaded into an 29.5 mm long section of unthreaded rigid PVC 3/8 pipe size with a 12.5 mm inner diameter and a 17.1 mm outer diameter compressed between two 11.9 mm phosphor bronze electrodes. Load was applied downward on the upper electrode incrementally up to pressures of 22.75 MPa. Pressure and resistivity were recorded at each step and plotted. Resistivity was measured using a DMM6500 Keithley Multimeter (Tektronix, Beaverton, OR, USA). Tests were repeated six times for each condition.

The level of accuracy for this proposed method is dependent upon the resolution of the graduated cylinder, the multimeter and the load cell; as the input mass does not change over time during testing, the accuracy with the equipment used here is expected to be  $\pm 100$  nV,  $\pm 10$  pA,  $\pm 1$   $\mu\Omega$ , and  $\pm 0.35$  MPa.

### 2.2.3. Compactibility

A third novel method, powder compactibility, was used to evaluate the feedstock powders in this study. This method is similar to ISO 3927 in that powders are compressed in a die and the strength and density of the green body is evaluated; however, in this method, a single rapidly applied load is used to compact the powder. Figure 11 shows a schematic of a cross section of the powder compaction method. A total of 0.03 mL (untapped) of powder was loaded into the support base with paper liner and enclosed with a 6.35 mm pin. Then, a rapidly applied blow of 1 MPa was applied to the pin. After the load was applied, the powder forms a coherent green body; Figure 12 shows an example of an aluminum

green body. Uncompacted powder was removed from the green body via light tapping and the weight of the green body was compared to the initial weight of the input powder. Thickness of the green body was also measured. Error bars for all methods are shown as standard error (square root of the standard deviation divided by the number of samples). Tests were completed six times for each sample.

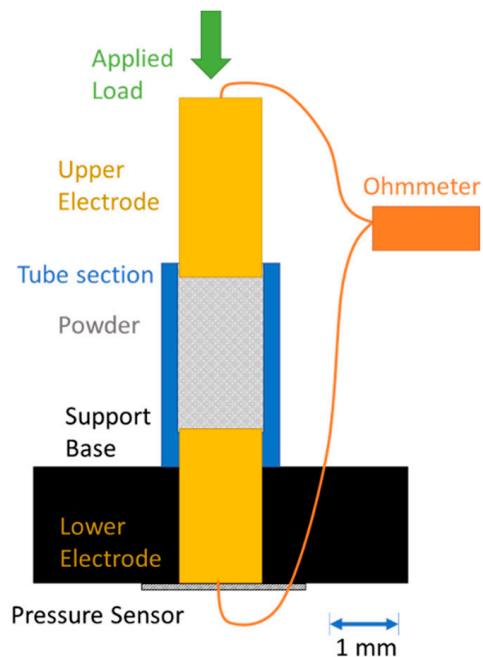


**Figure 10.** Schematic showing cross section of compressibility test; support base and ohmmeter not to scale.

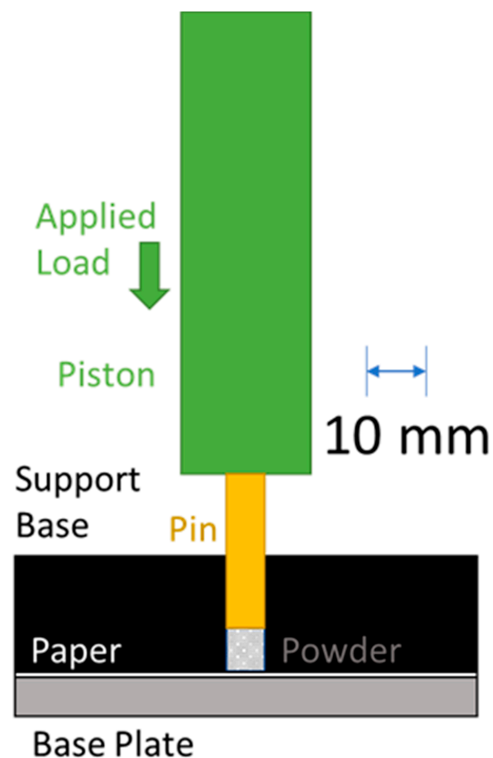


**Figure 11.** Schematic showing cross section of compactibility test.



**Figure 12.** Example of aluminum green body formed by compactibility testing.

The level of accuracy for this proposed method is dependent upon the resolution of the graduated cylinder, the scale, and micrometer; the accuracy with the equipment used here is expected to be  $\pm 1$  mL,  $\pm 0.0001$  g, and  $\pm 0.01$  mm.

#### 2.2.4. Cold Spray

The Cr powders were additionally evaluated via cold spray. Samples were consolidated using a high-pressure cold spray system (Gen III from VRC Metal Systems, Box Elder, SD, USA) using a He carrier gas at 575 °C and 3.6 MPa (525 psi), and deposits were built up onto a C2-Almen strip (SAE 1070 steel of HRc 44–50, 76.098 mm long by 18.987 mm wide by 2.410 mm thick) before cross sectioning and metallurgical preparation for imaging.

### 3. Results and Discussion

#### 3.1. Quality Control of Cermet Powder Blends

WIP-C1 and WIP-C2 chromium carbide-based powders share similar powder properties that can make them difficult to evaluate for quality control if not characterized using appropriate techniques. The two powders highlighted here have (1) nearly identical apparent and tapped density, (2) similar flowability values when measured using a Carney flow device, and (3) average particle sizes with D50 values within a few microns of one another. Table 7 shows a breakdown of values for each of these characteristics with the percent difference reported. The percent differences are less than 3% for each type of measurement listed. Additionally, both WIP-C1 and WIP-C2 are composed of the same three elements in slightly different concentrations. WIP-C1 is chrome-carbide nickel of composition Cr-31Ni-3C. WIP-C2 is chrome-carbide nickel-chrome of composition Cr-26Ni-3C. While measuring composition is a way to differentiate between these two powders, not all additive manufacturing facilities or laboratories have the in-house capabilities to conduct such testing and utilizing external testing facilities can be time consuming and expensive. For this case study, the percent mass compacted metric is highlighted as a method for detecting slight differences in soft phase composition, which have been shown to correlate to cold spray properties like deposition efficiency [19]. This method allows for much faster iteration and quality control than slower, more expensive methods such as compositional analysis.

Commercially available WIP-C1 and WIP-C2 samples were collected and evaluated using the powder impact device, which rapidly compacts samples using a known applied load. Five different lots of powder for each material type were tested. Each lot of powder was measured for percent mass compaction three times. Figure 13 shows the average percent of all measurements for each material and error bars representing standard error. The average percent mass compacted values for WIP-C1 and WIP-C2 were 35.2% and 23.9% respectively. This trend correlates with what is seen in cold spray; when deposited at the

same processing conditions, WIP-C2 has a deposition efficiency approximately 10–15% less than that of WIP-C1.

**Table 7.** Comparison of WIP-C1 and WIP-C2 powder properties.

Powder	D <sub>50</sub> (μm)	D <sub>50</sub> % dif.	Apparent Density (g/mL)	Apparent Density % dif.	Tapped Density (g/mL)	Tapped Density % dif.	Carney Flow (g/s)	Carney Flow % dif.
WIP-C1	28.0		3.93		4.40		17.3	
WIP-C2	30.7	2.3%	3.96	0.2%	4.47	0.4%	18.1	1.1%

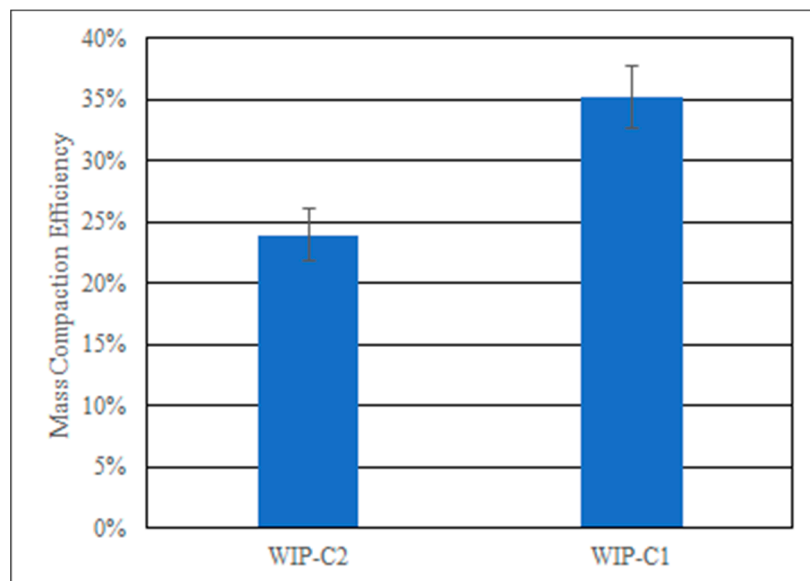


**Figure 13.** Percent mass compacted values for WIP-C1 and WIP-C2.

The higher percent mass compacted value and improved deposition efficiency in cold spray for WIP-C1 can be attributed to the higher nickel concentration of the powder. Nickel is ductile compared to the carbide it is blended with, and in cold spray and in this compaction method, the ductility and concentration of the binding agent (the nickel) in the powder effect how much of the material binds together when energy is applied; this is considered powder cohesion. Similar to cold spray, consolidation of the powder into a bulk compact due to the impacting load applied with this device causes plastic deformation of ductile materials. The chromium carbide in both materials does not plastically deform during impact. WIP-C1 has more nickel but less chromium content than WIP-C2. Because nickel is softer than chromium, a larger green body forms during compaction, which corresponds to a higher mass compacted value. The powder compactibility method demonstrated here provides additional information relating to the ductility of powder which is critical for additive manufacturing technologies such as cold spray. This technique can be used to assist in developing novel materials and act as a quality standard for validating conformance during powder manufacturing. This method is entirely novel in this particular application. Powder compaction methods typically utilize slowly and consistently applied loads, such as isostatic pressing, to create a green body, whereas with this method, the rapidly applied load mimics the underlying phenomena of cold spray, namely the high strain rate deformation. The advantage of using the powder compactibility method is the ability to screen powders for cold spray much faster than actually utilizing them in the cold spray process; this can help reduce development time as well as be used as a quality control metric.

### 3.2. Pre-Processing of Chromium Powder

The Cr powder evaluated in this study was of a less than 20  $\mu\text{m}$  size cut, which frequently results in low flowability and difficulty in cold spraying. Comparing the unprocessed Cr to the processed Cr powder, the size distribution and density data shown in Table 2 indicate no significant change in the d-values or density after processing. Additionally, when powder flowability is evaluated via standard Carney and Hall metrics, both powders produce a no-flow condition. Given this information, it might be predicted that the powders would behave similarly in cold spray. However, when the different Cr powders were cold sprayed under the same conditions, they resulted in different coating thicknesses and quality. Figure 14 shows optical micrographs of the coatings; it can be seen that the processed Cr has a more uniform and denser coating as well as a thicker build up in the same number of passes. Feedstock evaluation techniques that can indicate these potential differences prior to spraying can save time and development costs. With this in mind, the novel characterization methods proposed here were used to characterize the Cr powders.

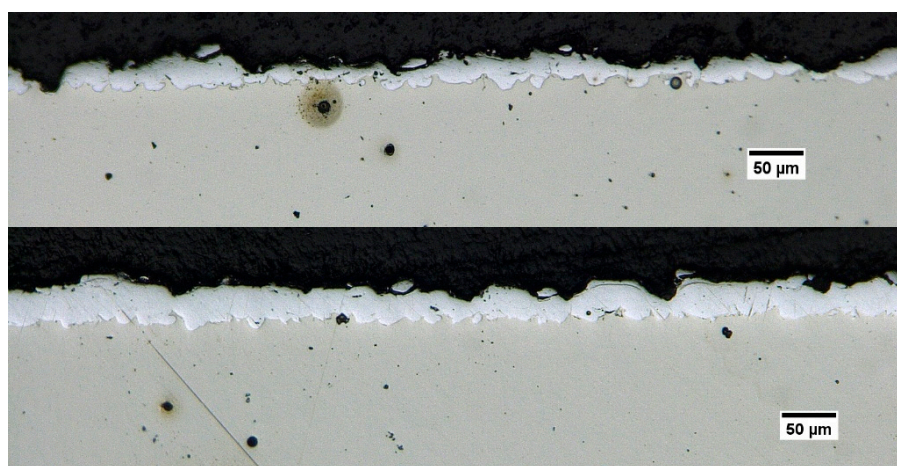


**Figure 14.** Optical micrographs showing cross sections of cold spray deposits for unprocessed Cr (top) and dried Cr (bottom).

Figure 15 indicates powder compressibility, showing powder resistivity as a function of applied pressure; it can be seen that little to no difference between the powders was measured via this method. Figures 16 and 17 show powder compactibility for each powder. This method provides the metrics of percent mass compaction and green body thickness, and differences in the powder can be seen in both metrics with the dried Cr compacting better than the unprocessed Cr. As was seen in the WIP-C1 powder, this correlates to improved deposition in cold spray due to the improved ductility, plastic deformation, and powder cohesion.

Additionally, the standard error for the dried Cr powder is much lower than that of the unprocessed Cr powder, and while improved repeatability may be an indicator of powder quality, additional work is needed. Table 8 shows the modified Hall flow data compared to the standard Carney and Hall flow data; only the modified Hall flow was able to discern a difference between the powders. Unlike the aluminum and wear powders also considered in this study, the Cr powder has an angular morphology and a much finer size distribution, both of which reduce its flowability and make it difficult to quantify. The improved flowability of the processed Cr seen over the unprocessed Cr powder seen in the vibrational Hall method is likely the driver of its improved coating quality. While the flow rate of the dried Cr powder was still slow, especially compared to the aluminum or wear powders also considered in this study, it flowed consistently and evenly throughout the testing time, a marked improvement over the standard Hall and Carney methods. In a cold spray system, this translates to consistent feeding, which would result in a more

uniform coating thickness. The advantage of using this modified flowability method is the ability to differentiate between powders that would otherwise be categorized as “no flow”, extending the measurement range and providing additional screening and quality control methods.

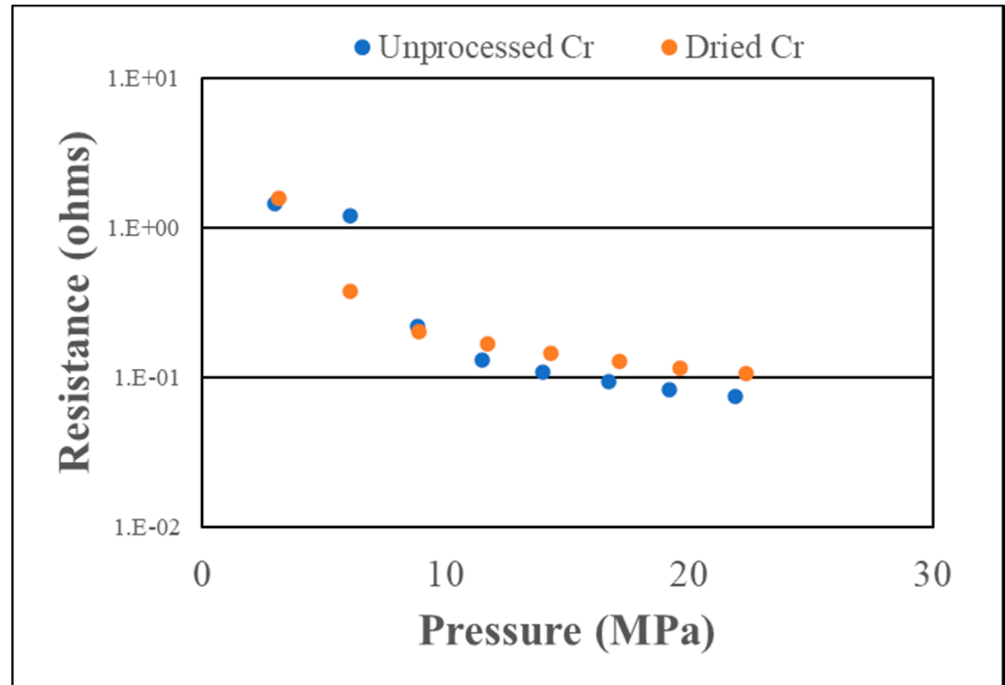


Figure 15. Powder compressibility data for evaluated Cr powders.

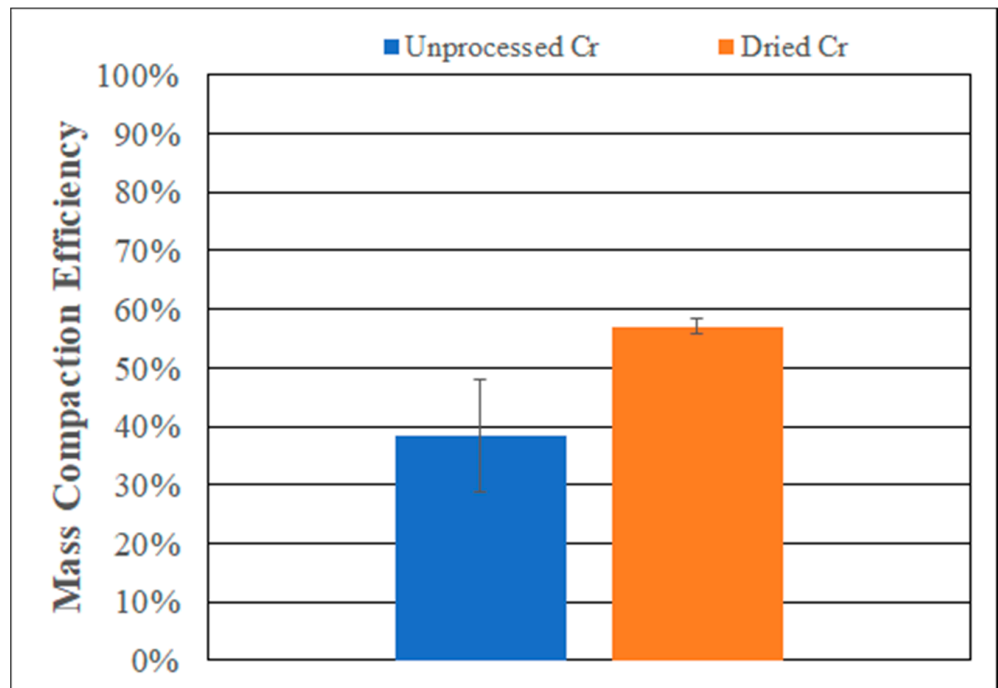


Figure 16. Percent mass compaction data of impacted green bodies for evaluated Cr powders.

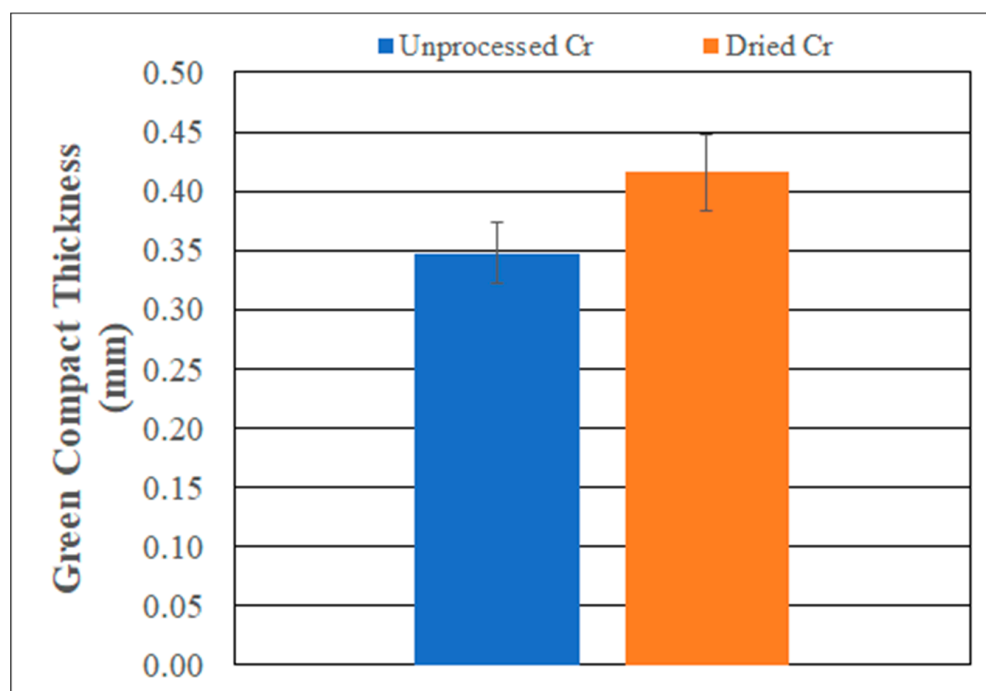


Figure 17. Green body thickness data of impacted green bodies for evaluated Cr powders.

Table 8. Standard and modified flowability data for Cr powders.

Powder	Standard Carney Flow Rate (g/s)	Standard Hall Flow Rate (g/s)	Vibrated Hall Flow Rate (g/s)
As-Received Cr	NF	NF	NF
Dried Cr	NF	NF	0.07 g/s

Overall, this case study demonstrates the benefits of utilizing a modified vibrational Hall flow method when considering fine powders of poor flowability and the benefits of utilizing powder compaction. Specifically, the addition of vibration to a flowability device allows for improved resolution on powder flowability, enabling data to be generated on powder that would otherwise simply be characterized as “No Flow” through traditional flowability methods. Additionally, the powder compaction metrics of percent mass compacted and green body thickness both indicate that the dried Cr compacts better than the unprocessed Cr, a relationship that is seen in the cold spray deposits.

### 3.3. Pre-Processing of Aluminum 6061

To isolate the effect of the processing conditions on aluminum powder characteristics, small batches of Aluminum 6061 powder were evaluated in high, medium, and low oxygen content conditions. Table 3 indicates that no significant changes to the size distribution or densities resulted from the processing. While measuring composition is a way to differentiate between these powders, not all additive manufacturing facilities or laboratories have the in-house capabilities to conduct such testing and utilizing external testing facilities can be time consuming and expensive. The methods used here aim to differentiate between the powders without needing to directly measure composition.

Figures 18 and 19 show how processing influenced the cohesive properties of the powder. The mass compaction (Figure 18) of the high oxygen powder (65.7%) fell short of the medium and low oxygen powders, but the medium oxygen (76.8%) and low oxygen (82.0%) powders remained too close to distinguish one parameter set from the other. The thickness of the resulting compacts (Figure 19) gave similar results, with the high oxygen powder forming thicker compacts with an average thickness of 0.58 mm

while the medium and low oxygen conditions both form pucks with an average thickness of 0.36 mm. Evaluating the powders' flow characteristics through Carney flow (Figure 20) also yielded little distinction between the high oxygen powder and the medium and low oxygen powders.

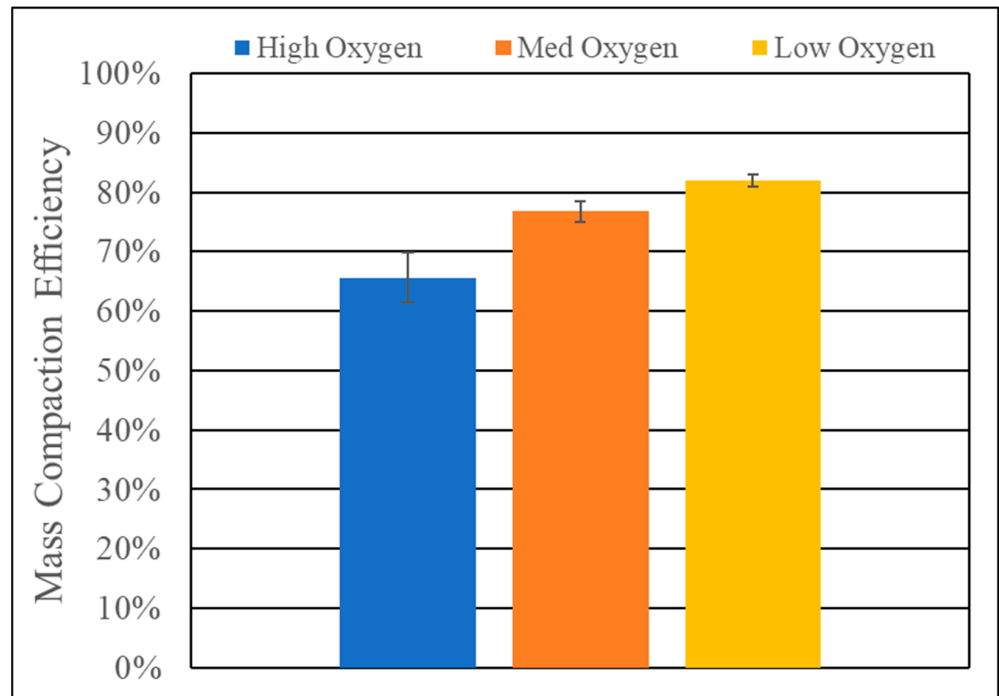


Figure 18. Percent mass compaction data of impacted green bodies for evaluated AL6061 powders.

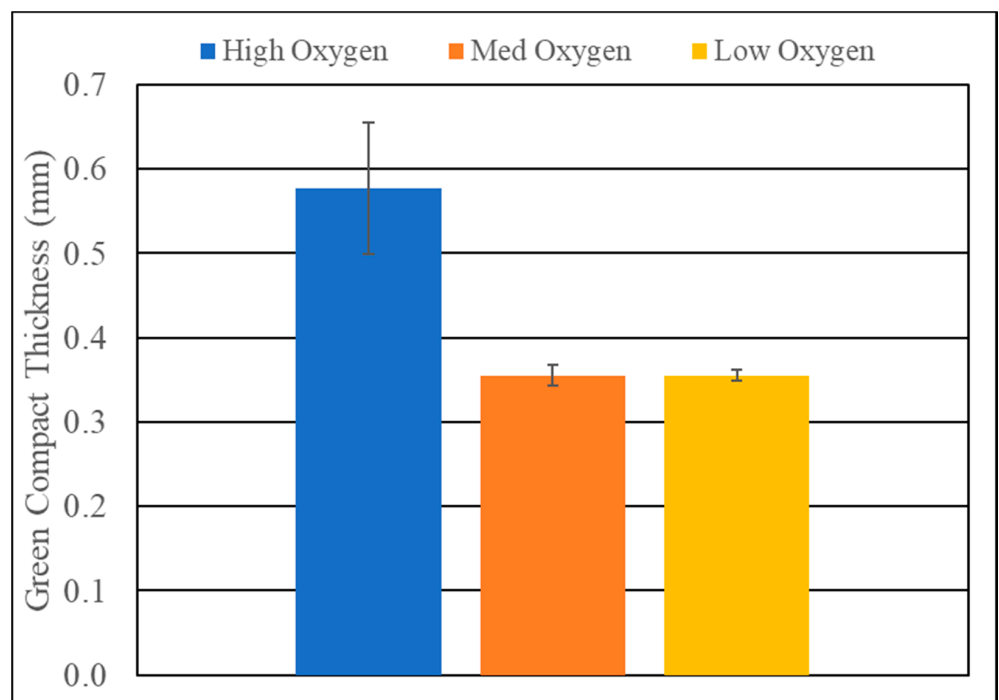


Figure 19. Green body thickness data of impacted green bodies for evaluated AL6061 powders.

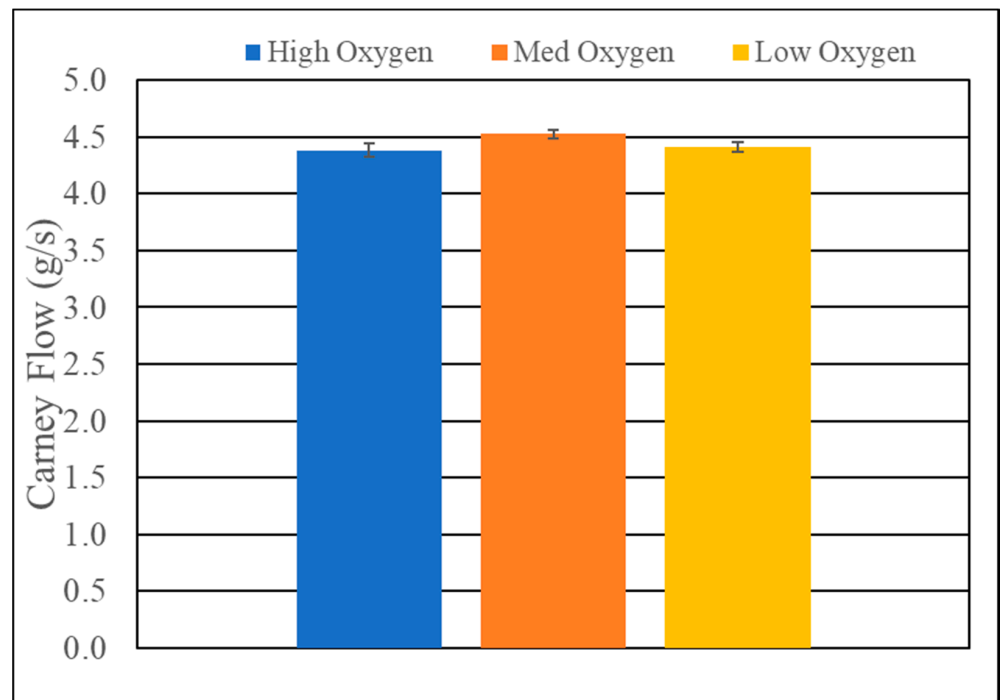


Figure 20. Carney flow data for evaluated AL6061 powders.

Figure 21 shows the compressibility curves of the three powders. The high oxygen powder was consistently one to two orders of magnitude of electrical resistance above the medium and low oxygen powders at any given pressure, and the medium oxygen powder was between the high and low oxygen powders. Figure 22 shows the final resistance measurement for the high and low oxygen powders, along with the standard error for both the resistance and pressure measurements. The high oxygen powder had a higher average resistance (989 ohms) than the low oxygen powder (134 ohms) under similar maximum forces. From these figures, a clear difference between the otherwise indiscernible powders can be identified.

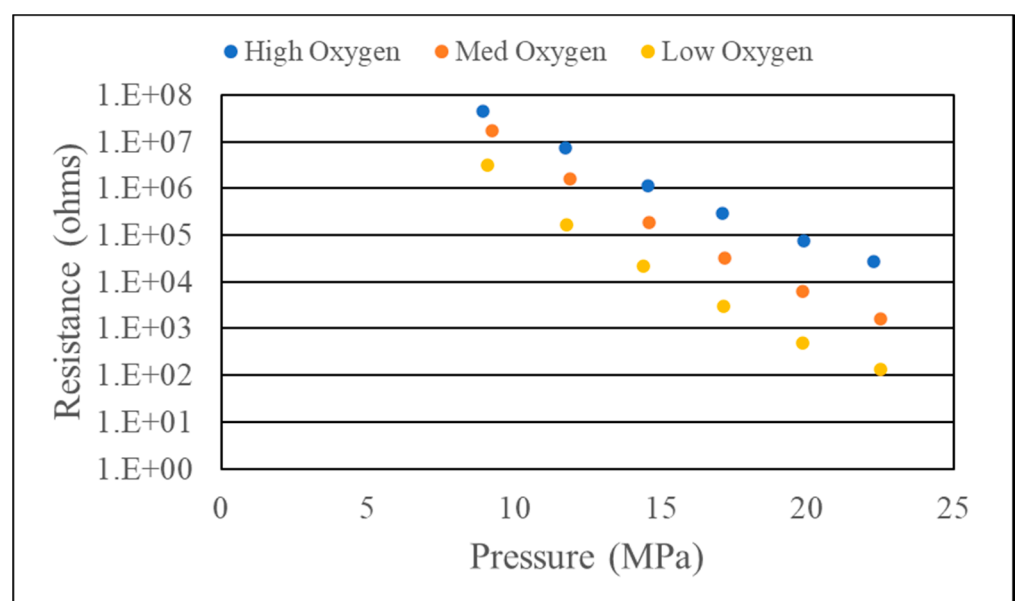
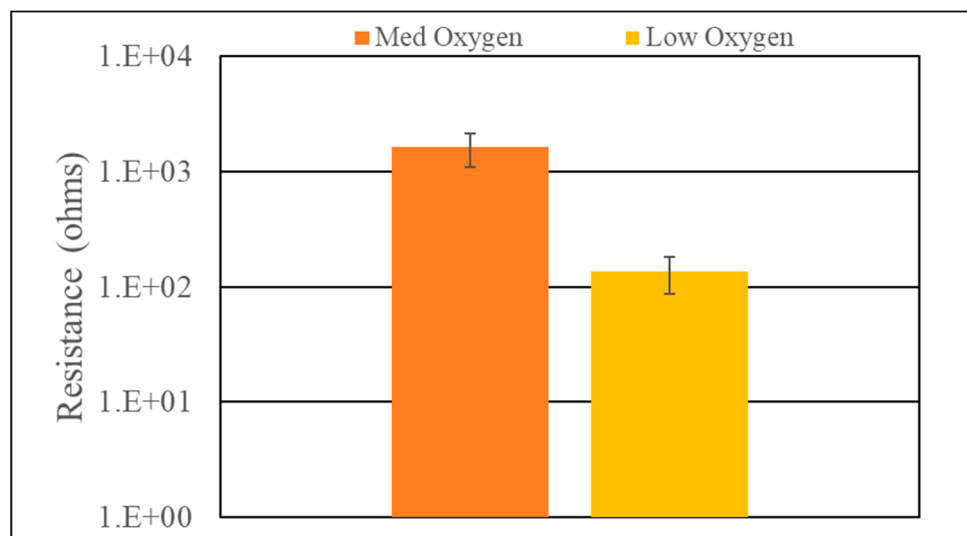


Figure 21. Compressibility data for the evaluated AL6061 powders.



**Figure 22.** Final resistance value with one standard error in resistance and pressure for med and low O<sub>2</sub> AL6061 powders.

This case study serves to highlight that, while powders can be produced with different oxygen contents that were similar in size, flow, and compaction metrics, they can be separated electrically. Given that powder compressibility has been tied to surface oxides and powder defects, both of which are generally negative relative to the cold spray process, having an understanding of the differences in these feedstock powders will enable users to have better quality control over their final part quality. It has been shown that processing of aluminum powders affects cold spray performance, but the characterization performed in these studies requires advanced techniques and only evaluates small sample sizes [33–35]. Powder compressibility can be performed on a relatively large sample of powder in a matter of minutes. Additional work is needed to correlate powder compressibility with microstructure and hardness, but it remains clear that compressibility can still be used to differentiate between conditions of otherwise similar aluminum powders. The advantage of using the powder compressibility method is the ability to screen powders for cold spray much faster than actually utilizing them in the cold spray process; this can help reduce development time as well as be used as a quality control metric.

#### 4. Conclusions

The case studies presented here highlight critical challenge points for the cold spray community and this study has demonstrated the utility of novel powder feedstock characterization methods in addressing these concerns. These metrics, namely powder compressibility, powder compactibility, and a modified vibrational flow, in addition to traditional techniques, such as size distribution, morphology, and chemistry, can differentiate between key feedstock features. The chrome carbide case study demonstrated the ability of powder compactibility to differentiate between binder content in two otherwise similar (size and flowability) powders. The processing of Cr powder case study demonstrated the ability of the vibrational Hall method and powder compaction to differentiate between powders that would otherwise be considered identical for all other attributes including composition and size. Finally, the processing of aluminum case study demonstrated the ability of powder compressibility to differentiate between oxygen levels in three powders, providing a level of quality control missed by only evaluating size and flowability. When correlated to consolidated properties, these metrics can be used to create standards and for quality control. When standards have been developed, these methods can serve as a rapid screening tool during novel powder development, decreasing overall development time.

**Author Contributions:** Conceptualization, B.Y., J.H. and C.W.; Data curation, B.Y. and J.H.; Formal analysis, B.Y., J.H. and C.W.; Funding acquisition, M.S., C.W. and A.B.; Investigation, B.Y., J.H., S.L. and C.W.; Methodology, B.Y., J.H. and C.W.; Project administration, M.S., C.W. and A.B.; Resources, C.W., M.S., and A.B.; Supervision, M.S., C.W. and A.B.; Validation, B.Y.; Visualization, B.Y., J.H., S.L. and C.W.; Writing original draft, B.Y., J.H., S.L. and C.W.; Writing review and editing, B.Y., J.H., S.L., M.S., C.W. and A.B. All authors have read and agreed to the published version of the manuscript.

**Funding:** This work was funded by the United States Army Research Laboratory, grant # W911NF-19-2-0155.

**Institutional Review Board Statement:** Not applicable.

**Informed Consent Statement:** Not applicable.

**Data Availability Statement:** All data are available in the main text.

**Conflicts of Interest:** The authors declare no conflict of interest. The funders had no role in the design of the study; in the collection, analyses, or interpretation of data; in the writing of the manuscript, or in the decision to publish the results.

## References

1. Abdulhameed, O.; Al-Ahmari, A.; Ameen, W.; Mian, S.H. Additive manufacturing: Challenges, trends, and applications. *Adv. Mech. Eng.* **2019**, *11*. [[CrossRef](#)]
2. Gao, W.; Zhang, Y.; Ramanujan, D.; Ramani, K.; Chen, Y.; Williams, C.B.; Wang, C.C.; Shin, Y.C.; Zhang, S.; Zavattieri, P.D. The status, challenges, and future of additive manufacturing in engineering. *Comput.-Aided Des.* **2015**, *69*, 65–89. [[CrossRef](#)]
3. Gong, X.; Anderson, T.; Chou, K. Review on powder-based electron beam additive manufacturing technology. *Manuf. Rev.* **2014**, *1*, 2. [[CrossRef](#)]
4. Frazier, W.E. Metal additive manufacturing: A review. *J. Mater. Eng. Perform.* **2014**, *23*, 1917–1928. [[CrossRef](#)]
5. Ngo, T.D.; Kashani, A.; Imbalzano, G.; Nguyen, K.T.Q.; Hui, D. Additive manufacturing (3D printing): A review of materials, methods, applications and challenges. *Compos. Part B Eng.* **2018**, *143*, 172–196.
6. Guo, N.; Leu, M.C. Additive manufacturing: Technology, applications and research needs. *Front. Mech. Eng.* **2013**, *8*, 215–243. [[CrossRef](#)]
7. Heiden, M.J.; Deibler, L.A.; Rodelas, J.M.; Koepke, J.R.; Tung, D.J.; Saiz, D.J.; Jared, B.H. Evolution of 316L stainless steel feedstock due to laser powder bed fusion process. *Addit. Manuf.* **2019**, *25*, 84–103. [[CrossRef](#)]
8. Deputy Director for Strategic Technology Protection and Exploitation. Department of Defense Additive Manufacturing Strategy. [Online]. Available online: <https://www.cto.mil/wp-content/uploads/2021/01/dod-additive-manufacturing-strategy.pdf> (accessed on 24 February 2021).
9. US Dept of Energy. Advanced Manufacturing Office Multi-Year Program Plan. Available online: [https://www.energy.gov/sites/prod/files/2017/01/f34/DraftAdvancedManufacturingOfficeMYPP\\_1.pdf](https://www.energy.gov/sites/prod/files/2017/01/f34/DraftAdvancedManufacturingOfficeMYPP_1.pdf) (accessed on 24 February 2021).
10. US Food & Drug Administration. Technical Considerations for Additive Manufactured Medical Devices Guidance for Industry and Food and Drug Administration Staff Preface Public Comment. Available online: <https://www.fda.gov/media/97633/download> (accessed on 24 February 2021).
11. Additive Manufacturing | NIST. National Institute of Standards and Technology. Available online: <https://www.nist.gov/additive-manufacturing> (accessed on 24 February 2021).
12. Muñiz-Lerma, J.A.; Nommeots-Nomm, A.; Waters, K.E.; Brochu, M. A comprehensive approach to powder feedstock characterization for powder bed fusion additive manufacturing: A case study on AlSi7Mg. *Materials* **2018**, *11*, 2386. [[CrossRef](#)] [[PubMed](#)]
13. Champagne, V.K. *The Cold Spray Materials Deposition Process*, 1st ed.; Woodhead Publishing: Cambridge, UK, 2007.
14. ASTM B964-16. *Standard Test Methods for Flow Rate of Metal Powders Using the Carney Funnel*; ASTM International: West Conshohocken, PA, USA, 2016. Available online: [www.astm.org](http://www.astm.org) (accessed on 31 March 2021).
15. ASTM B213-20. *Standard Test Methods for Flow Rate of Metal Powders Using the Hall Flowmeter Funnel*; ASTM International: West Conshohocken, PA, USA, 2020. Available online: [www.astm.org](http://www.astm.org) (accessed on 31 March 2021).
16. ASTM F3049-14. *Standard Guide for Characterizing Properties of Metal Powders Used for Additive Manufacturing Processes*; ASTM International: West Conshohocken, PA, USA, 2014. Available online: [www.astm.org](http://www.astm.org) (accessed on 31 March 2021).
17. MIL-DTL-32495. *Detail Specification: Aluminum-Based Powders for Cold Spray Deposition*; Department of Defense: Washington, DC, USA, 2014.
18. Khalkhali, Z.; Rothstein, J.P. Characterization of the cold spray deposition of a wide variety of polymeric powders. *Surf. Coat. Technol.* **2020**, *383*, 125251. [[CrossRef](#)]
19. Heelan, J.; Langan, S.M.; Walde, C.; Nardi, A.; Siopis, M.; Barth, R.; Landry, T.; Birt, A. Effect of WC-Ni Powder Composition and Preparation on Cold Spray Performance. *Coatings* **2020**, *10*, 1196. [[CrossRef](#)]

20. DeForce, B.; Eden, T.; Potter, J.; Champagne, V.; Leyman, P.; Helfritsch, D. Application of aluminum coatings for the corrosion protection of magnesium by cold spray. In Proceedings of the Tri-Service Corrosion Conference, Denver, CO, USA, 3–6 December 2007. Available online: <https://citeseerx.ist.psu.edu/viewdoc/download?doi=10.1.1.523.4800&rep=rep1&type=pdf> (accessed on 31 March 2021).
21. Montes, J.M.; Cuevas, F.G.; Cintas, J. Electrical Resistivity of Metal Powder Aggregates. *Metall. Mater. Trans. B* **2007**, *38*, 957–964. [[CrossRef](#)]
22. Montes, J.M.; Cuevas, F.G.; Cintas, J. Electrical resistivity of a titanium powder mass. *Granul. Matter* **2011**, *13*, 439–446. [[CrossRef](#)]
23. Barroso-Bogeat, A.; Alexandre-Franco, M.; Fernández-González, C.; Macías-García, A.; Gómez-Serrano, V. Electrical conductivity of activated carbon–metal oxide nanocomposites under compression: A comparison study. *Phys. Chem. Chem. Phys.* **2014**, *16*, 25161–25175. [[CrossRef](#)]
24. Hemeda, A.A.; Zhang, C.; Hu, X.Y.; Fukuda, D.; Cote, D.; Nault, I.M.; Nardi, A.; Champagne, V.K.; Ma, Y.; Palko, J.W. Particle-based simulation of cold spray: Influence of oxide layer on impact process. *Addit. Manuf.* **2021**, *37*, 101517. [[CrossRef](#)]
25. Ichikawa, Y.; Tokoro, R.; Tanno, M.; Ogawa, K. Elucidation of cold-spray deposition mechanism by auger electron spectroscopic evaluation of bonding interface oxide film. *Acta Mater* **2019**, *164*, 39–49. [[CrossRef](#)]
26. Decost, B.L.; Jain, H.; Rollett, A.D. Computer Vision and Machine Learning for Autonomous Characterization of AM Powder Feedstock. *JOM* **2017**, *69*, 456–465. [[CrossRef](#)]
27. Sousa, B.C.; Gleason, M.A.; Haddad, B.; Champagne, V.K.; Nardi, A.T.; Cote, D.L. Nanomechanical Characterization for Cold Spray: From Feedstock to Consolidated Material Properties. *Metals* **2020**, *10*, 1195. [[CrossRef](#)]
28. Silvello, A.; Cavaliere, P.D.; Albaladejo, A.; Martos, A.; Dosta, S.; Cano, I.G. Powder Properties and Processign Conditions Affecting Cold Spray Deposition. *Coatings* **2020**, *10*, 91. [[CrossRef](#)]
29. Tsaknopoulos, K.; Walde, C.; Tsaknopoulos, D.; Champagne, V.; Cote, D. Characterization of Thermally Treated Gas-Atomized Al 5056 Powder. *Materials* **2020**, *13*, 4051. [[CrossRef](#)]
30. Valent, R.C.; Ostapenko, A.; Sousa, B.C.; Grubbs, J.; Massar, C.J.; Cote, D.B.; Neamtu, R. Classifying Powder Flowability for Cold Spray Additive Manufacturing Using Machine Learning. In Proceedings of the 2nd International Workshop on Big Data Tools, Methods, and Use Cases for Innovative Scientific Discovery, IEEE BigData Conference, Virtual, Atlanta, GA, USA, 10–13 December 2020.
31. ISO 13322-1. *Particle Size Analysis—Image Analysis Methods—Part 1: Static Image Anlaysis Methods*; International Standards Organization: Geneva, Switzerland, 2014.
32. ASTM B527-20. *Standard Test Method for Tap Density of Metal Powders and Compounds*; ASTM International: West Conshohocken, PA, USA, 2020. Available online: [www.astm.org](http://www.astm.org) (accessed on 31 March 2021).
33. Story, W.A.; Brewer, L.N. Heat Treatment of Gas-Atomized Powders for Cold Spray Deposition. *Metall. Mater. Trans. A* **2018**, *49*, 446–449. [[CrossRef](#)]
34. Hall, A.C.; Cook, D.J.; Neiser, R.A.; Roemer, T.J.; Hirschfeld, D.A. The effect of a simple annealing heat treatment on the mechanical properties of cold-sprayed aluminum. *J. Therm Spray Technol* **2006**, *15*, 233–238. [[CrossRef](#)]
35. Sabard, A.; McNutt, P.; Begg, H.; Hussain, T. Cold spray deposition of solution heat treated, artificially aged and naturally aged Al 7075 powder. *Surf. Coat. Technol.* **2020**, *385*, 125367. [[CrossRef](#)]